

Fate of entanglement in magnetism under Lindbladian or non-Markovian dynamics and conditions for their transition to Landau-Lifshitz-Gilbert classical dynamics

Federico Garcia-Gaitan  and Branislav K. Nikolić ^{*}

Department of Physics and Astronomy, University of Delaware, Newark, Delaware 19716, USA



(Received 1 May 2023; revised 18 April 2024; accepted 29 April 2024; published 16 May 2024)

The entanglement of many localized spins (LSs) within solid magnetic materials is a topic of great basic and applied interest, particularly after becoming amenable to experimental scrutiny where recent neutron scattering experiments have witnessed macroscopic entanglement in the ground state (GS) of antiferromagnets persisting even at elevated temperatures. On the other hand, spintronics and magnonics studies assume that LSs of antiferromagnets are in unentangled Néel GS, as well as that they evolve, when pushed out of equilibrium by current or external fields, according to the Landau-Lifshitz-Gilbert (LLG) equation viewing LSs as classical vectors of *fixed* length. The prerequisite for applicability of the LLG equation is *zero entanglement* in the underlying many-body quantum state of LSs. In this study, we initialize quantum Heisenberg ferro- or antiferromagnetic chains hosting $S = 1/2$, $S = 1$, or $S = 5/2$ LSs into an unentangled pure state and then evolve them by quantum master equations (QMEs) of Lindblad or non-Markovian type, derived by coupling LSs weakly to a bosonic bath (due to phonons in real materials) or by using additional “reaction coordinate” in the latter case. The time evolution is initiated by applying an external magnetic field, and entanglement of the ensuing *mixed* quantum states is monitored by computing its negativity. We find that non-Markovian dynamics *never* brings entanglement to zero, in the presence of which the vector of spin expectation value *changes its length* to render the LLG equation *inapplicable*. Conversely, Lindbladian (i.e., Markovian) dynamics ensures that entanglement goes to 0, thereby enabling quantum-to-classical transition in all cases— $S = 1/2$, $S = 1$, and $S = 5/2$ ferromagnets or $S = 5/2$ antiferromagnets—*except* for $S = 1/2$ and $S = 1$ antiferromagnets. Finally, we investigate the stability of an entangled antiferromagnetic GS upon suddenly coupling it to bosonic baths.

DOI: [10.1103/PhysRevB.109.L180408](https://doi.org/10.1103/PhysRevB.109.L180408)

Introduction. The fate of entanglement of many interacting quantum spins, localized at the sites of crystalline lattices of magnetic materials [1] or in optical lattices of their quantum simulators [2], under finite temperature or nonequilibrium conditions is a topic of great contemporary interest. For example, recent experiments [3–5] have succeeded in witnessing [6–8] multipartite entanglement [3,9] of macroscopically large numbers of spins hosted by antiferromagnetic insulators (AFIs) in equilibrium up to surprisingly high temperatures of $T \lesssim 200$ K [3]. Transient entanglement in nonequilibrium AFIs could also be witnessed via very recently proposed schemes [10,11]. Due to finite temperature and/or nonequilibrium, such systems inevitably generate *mixed entangled* states, also in the focus of our study [Eq. (2)]. Such quantum states are far less understood [12–16] than the pure [2] entangled ones. In computational quantum physics, quantum spin systems are a standard playground for developing algorithms, such as tensor networks (TNs) [17], that can efficiently encode ground states (GSs) containing low-entanglement—however, entanglement growth in nonequilibrium [18] poses a significant challenge for these algorithms [19] and the role of dissipative environment in limiting the so-called “entanglement barrier” is intensely explored [20].

It is insightful to invoke a pedagogical example of an entangled GS, such as that of an AFI chain hosting localized

spins (LSs) $S = 1/2$, which has been realized experimentally [21] and is described by the Heisenberg Hamiltonian [22]

$$\hat{H}_H = J \sum_{i=1}^{N-1} \hat{\mathbf{S}}_i \cdot \hat{\mathbf{S}}_{i+1}. \quad (1)$$

The GS is entangled [9] as it cannot be expressed as the direct product of multiple single-spin states in any basis, as obvious from its form for $N = 4$ sites: $|\text{GS}\rangle_{\text{AFI}} = \frac{1}{\sqrt{12}}(2|\uparrow\downarrow\uparrow\downarrow\rangle + 2|\downarrow\uparrow\downarrow\uparrow\rangle - |\uparrow\uparrow\downarrow\downarrow\rangle - |\uparrow\downarrow\downarrow\uparrow\rangle - |\downarrow\downarrow\uparrow\uparrow\rangle - |\downarrow\uparrow\uparrow\downarrow\rangle)$. Its energy, ${}_{\text{AFI}}\langle\text{GS}|\hat{H}|\text{GS}\rangle_{\text{AFI}} = -2J$, is lower than the energy, $\langle\text{Néel}|\hat{H}|\text{Néel}\rangle = -J$, of an unentangled Néel state, $|\text{Néel}\rangle = |\uparrow\downarrow\uparrow\downarrow\rangle$, which is the precise meaning behind “quantum spin fluctuations” [23] *sintagma*. Here $\hat{S}_i^\alpha = \hat{I}_1 \otimes \dots \otimes S\hat{\sigma}^\alpha \otimes \dots \otimes \hat{I}_{N_{\text{AFI}}}$ acts nontrivially, as the Pauli matrix $\hat{\sigma}^\alpha$, in the Hilbert space of spin at site i ; \hat{I}_i is the unit operator; and $J > 0$ is an antiferromagnetic exchange interaction. The expectation value of spin, $\langle\hat{S}_i\rangle = \langle\text{GS}|\hat{S}_i|\text{GS}\rangle \equiv 0$, vanishes as a direct consequence [24–26] of the nonzero entanglement entropy of the AFI GS.

In the case of ferromagnetic insulators (FIs), quantum spin fluctuations [23] are absent [27] and both classical $\uparrow\uparrow\dots\uparrow\uparrow$ and its unentangled quantum counterpart $|\uparrow\uparrow\dots\uparrow\uparrow\rangle$ are GSs of the respective classical and quantum Hamiltonians. However, excited states of the FI chain—such as the one-magnon Fock state [28,29] $|1_q\rangle = \frac{1}{\sqrt{N}} \sum_{n=0}^{N-1} e^{iqx_n} |\underbrace{\uparrow\dots\uparrow}_n \downarrow_{N-n-1}\rangle$, where q is the wave vector and $x_n = na$ is the x

^{*}bnikolic@udel.edu

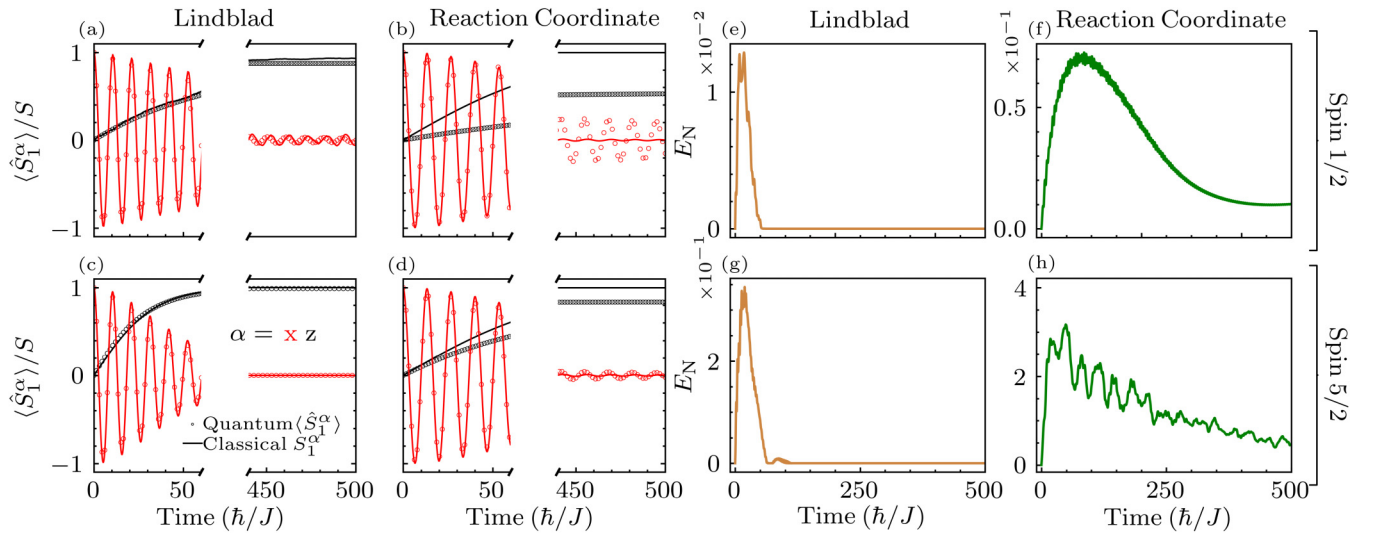


FIG. 1. Time dependence of QME-computed $\langle \hat{S}_i^\alpha(t) \rangle$ vs classical-LLG-computed $S_i^\alpha(t)$ of LSs (a), (b) $S = 1/2$ or (c), (d) $S = 5/2$ on site $i = 1$ of the FI chain of $N = 4$ sites. (e)–(h) Time dependence of entanglement negativity $E_N(t)$ [Eq. (11)] between two halves of the FI chain in the case of quantum evolution (circles) in panels (a)–(d), respectively. The time evolution of open quantum system of LSs is computed using either Lindblad (i.e., Markovian) or RC (i.e., non-Markovian) QME with the bosonic bath temperature $T = |J|$.

coordinate along the chain (with the lattice constant a)—are macroscopically entangled [30,31]. This is also the case of multimagnon states [32]. The robustness of entanglement of such states has been studied for a long time in quantum computing (using analogous multiqubit states known as W states) [16,33], as well as more recently in “quantum magnonics” [29] using quantum master equations (QMEs) formulated in the formalism of second quantization [34,35]. The single and multi-magnon states of AFIs are also entangled [36].

On the other hand, it is commonly assumed in antiferromagnetic spintronics [37–41] that the GS of an AFI is an unentangled Néel state; as well as that excited states (like magnons [42,43]) of either an AFI or a FI, as triggered experimentally by injected current [41,44,45] or electromagnetic radiation [46–52], are *classical and governed* [44,46,47,51–58] by the celebrated Landau-Lifshitz-Gilbert (LLG) equation [59–61]. It is also widely believed that a large spin value S [24] and/or room temperature ensure applicability of the LLG equation. This plausible notion is motivated by the eigenvalue of the \hat{S}_i^2 operator being $S^2(1 + 1/S)$, instead of S^2 , which suggests that quantum effects become progressively less important for $S > 1$. However, even for a single quantum spin the required value of S to match quantum and classical LLG dynamics can be unrealistically large [62,63] in the presence of magnetic anisotropy (or any quadratic or higher-order terms in the spin Hamiltonian) [64]. Also, quantum corrections persist for all $S < \infty$ [62,63], vanishing as $(2S)^{-1}$ in the classical limit [65]. Importantly, most of the standard magnetic materials host LSs with rather small $S \leq 5/2$ [66].

The search for a rigorous proof that quantum dynamics of a *single* spin can transition to classical LLG dynamics, due to interaction with a dissipative environment like the bosonic bath and conditions imposed on it, has a long history dating back to the archetypical spin-boson model [67] and recent generalizations [68] completing the proof while also unraveling the nature of quantum corrections to classical LLG dynamics. However, such proofs [68] do not explain how

quantum dynamics of *many* spins can transition to classical dynamics to be describable by a system of coupled LLG equations [69], often applied without scrutiny to both ferro- and antiferromagnets in spintronics [44] and magnonics [70]. The *key prerequisite* for such a transition is the *absence of entanglement* [24,25]; i.e., the underlying quantum state of many LSs must remain unentangled pure $|\sigma_1(t)\rangle \otimes |\sigma_2(t)\rangle \otimes \dots \otimes |\sigma_N(t)\rangle$ or unentangled mixed [12–16]

$$\hat{\rho}(t) = \sum_n p_n \hat{\rho}_n^{(1)}(t) \otimes \hat{\rho}_n^{(2)}(t) \dots \hat{\rho}_n^{(N)}(t), \quad (2)$$

at all times t in order for time evolution of quantum-mechanical expectation values $\langle \hat{S}_i \rangle$ to be able to transition to the solutions [69] $\mathbf{S}_i(t)$ of coupled LLG equations:

$$\langle \hat{S}_i \rangle(t) \mapsto \mathbf{S}_i(t). \quad (3)$$

Otherwise, in the entangled quantum state the length of vectors $\langle \hat{S}_i \rangle(t)$ is changing in time [71] which obviously *cannot be mimicked* by $\mathbf{S}_i(t)$ of *fixed length* [69] in the LLG equation. In Eq. (2), $\hat{\rho}_n^{(i)}$ is the density matrix of spin at site i . We consider usage of the LLG equation in the context of atomistic spin dynamics (ASD) [69], where each atom of the lattice hosts one classical vector \mathbf{S}_i .

In this Letter, we view AFIs and FIs as open quantum systems [72–74] by coupling them either (i) weakly to a bosonic bath, assumed to arise due to bosonic quasiparticles in solids such as phonons, whose tracing out allows one to derive [75] the universal Lindblad QME [Eq. (6)], or (ii) strongly to a single bosonic mode which, in turn, interacts weakly with the bosonic bath, so that tracing over both allows us to derive a non-Markovian QME within the so-called “reaction coordinate” (RC) method [76]. We monitor the presence of entanglement in the density matrix of all LSs $\hat{\rho}(t)$ via the entanglement negativity $E_N(t)$ [12–16], and we concurrently compare quantum $\langle \hat{S}_i \rangle(t)$ vs classical $\mathbf{S}_i(t)$ trajectories in Figs. 1–3.

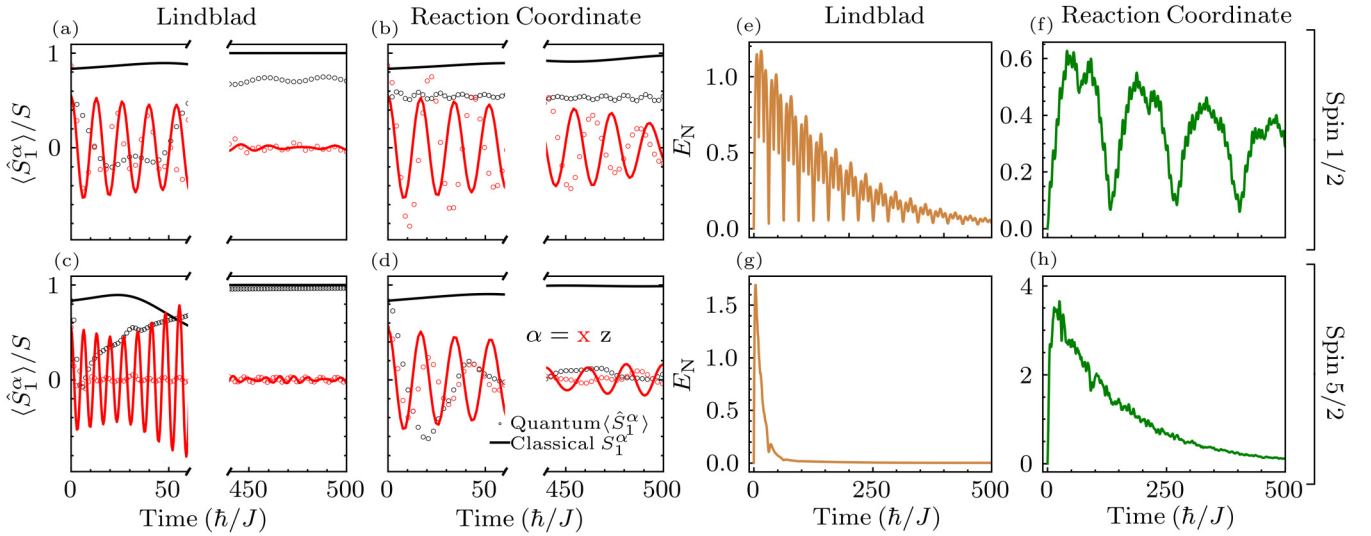


FIG. 2. Panels (a)–(h) are counterparts of Figs. 1(a)–1(h), but using an AFI chain composed of $N = 4$ sites. Additional cases of AFI or FI chains hosting $S = 1$ LSs, or including their additional interactions (such as easy-axis anisotropy, long-ranged dipole-dipole interaction, and Dzyaloshinskii-Moriya interaction), are provided in the SM [87].

Models and methods. We consider FI ($J < 0$) or AFI ($J > 0$) chain modeled by the Heisenberg Hamiltonian \hat{H}_H [Eq. (1)], which can include interaction with a homogeneous external magnetic field switching on for $t \geq 0$,

$$\hat{H} = \hat{H}_H - \sum_i g\mu_B \mathbf{B}_{\text{ext}}(t \geq 0) \cdot \hat{\mathbf{S}}_i, \quad (4)$$

where g is electron g -factor and μ_B is the Bohr magneton. We set $\hbar = 1$ and $k_B = 1$. These models of realistic magnetic

materials [3,21] are made open quantum systems by coupling them with bosonic baths, so that the total Hamiltonian becomes

$$\hat{H}_{\text{tot}} = \hat{H} + \hat{H}_{\text{bath}} + \hat{V}. \quad (5)$$

Here \hat{H}_{bath} models a set of independent baths, one per each spin [75,77], as harmonic oscillators [67], $\hat{H}_{\text{bath}} = \sum_{ik} w_{ik} \hat{a}_{ik}^\dagger \hat{a}_{ik}$, using an operator $\hat{a}_{ik} (\hat{a}_{ik}^\dagger)$ which annihilates (creates) a boson in mode k . The boson interacts with the spin operator at site i [72] via $\hat{V} = \sum_k g_k \sum_i \hat{\mathbf{S}}_i (\hat{a}_{ik} + \hat{a}_{ik}^\dagger)$, where g_k are the coupling constants. By assuming small g_k , a QME of the Lindblad type [78,79] can be derived by tracing out the bosonic bath and by expanding the resulting equation to second order. Rather than relying on traditional approaches for the derivation of the Lindblad QME—such as using Born, Markov, and secular approximations [76,78,80]—we follow the procedure of Ref. [75] for the universal Lindblad QME which evades difficulties of the secular approximation [81]. For example, for systems with (nearly) degenerate eigenenergies, as is the case of the FI and AFI models we consider, secular approximation leads to an improperly derived [80] Lindblad QME for LSs because of assuming that energy splitting is much bigger than fluctuations due to the bath. The same problem has been addressed in a number of recent studies [82,83], besides the resolution offered in Ref. [75].

The universal Lindblad QME [75] considers a single Lindblad operator \hat{L}_i for each spin, so that only N such operators are needed to obtain

$$d\hat{\rho}/dt = -i[\hat{H}, \hat{\rho}] + \sum_i \hat{L}_i \hat{\rho} \hat{L}_i^\dagger - \frac{1}{2} \{ \hat{L}_i^\dagger \hat{L}_i, \hat{\rho} \}, \quad (6)$$

where we also ignore typically negligible Lamb-shift corrections [76] to the Hamiltonian. The Lindblad QME is time-local due to the assumption that bath-induced changes to the system dynamics are slow relative to the typical correlation time of the bath. We compute \hat{L}_i operators as a power

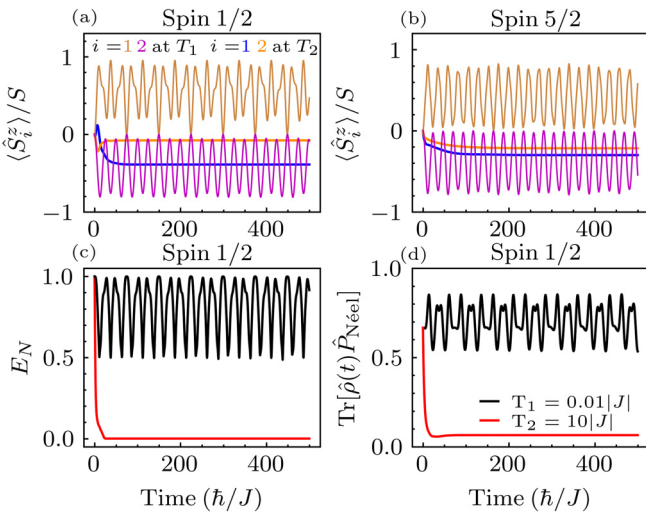


FIG. 3. Time dependence of (a), (b) spin expectation values at sites $i = 1$ and 2, (c) entanglement negativity $E_N(t)$ [Eq. (11)] between two halves of the AFI chain, and (d) overlap between the chain density matrix $\hat{\rho}(t)$ and pure states in the Néel subspace. The AFI chain has $N = 4$ sites, as well as an impurity introducing the z -axis anisotropy at site $i = 1$ [Eq. (12)]. The Lindblad equation (6) evolves $\hat{\rho}(t)$ upon coupling the AFI chain to the bosonic bath at $t = 0$, starting from the pure entangled GS but exhibiting Néel “checkerboard” order $\langle \hat{S}_i^z \rangle = -\langle \hat{S}_{i+1}^z \rangle \neq 0$ [26].

series (where we use the cutoff $N_L \leq 20$),

$$\hat{L}_i = \sum_{n=0}^{N_L} c_n (\text{ad}_{\hat{H}})^n [\hat{S}_i], \quad c_n = \frac{(-i)^n}{n!} \int_{-\infty}^{\infty} dt g(t) t^n, \quad (7)$$

thereby evading the need for exact diagonalization [75] of FI or AFI Hamiltonians. Here $\text{ad}_{\hat{H}}[X] = [\hat{H}, X]$ and the jump correlator function is defined via the Fourier transform of the spectral function of the bath, $J(\omega) = 2\pi \sum \delta(\omega - \omega_k)$, as $g(t) = \frac{1}{\sqrt{2\pi}} \int_{-\infty}^{\infty} d\omega \sqrt{J(\omega)} e^{-i\omega t}$. For numerical calculations, we considered an Ohmic [68] spectral function with a rigid ultraviolet cutoff,

$$J(\omega) = \frac{\Gamma\omega}{\omega_m} n_{\text{BE}}(\omega) \Theta(\omega_m - \omega), \quad (8)$$

where Γ is the reorganization energy representing the magnitude of fluctuations and dissipation, ω_m characterizes how quickly the bath relaxes towards equilibrium, $n_{\text{BE}}(\omega)$ is the Bose-Einstein distribution, and Θ is the Heaviside step function.

The Lindblad QME [Eq. (6)] is only valid for a weak system-bath coupling, as it assumes a second-order truncation

in g_k . Since this is not always the case, several approaches [72,74] exist to treat strong system-bath coupling, such as polaron, star-to-chain, and thermofield transformations [84], as well as the RC method [81]. The RC method we employ is based on the Bogoliubov transformation, and it allows one to construct a new bosonic mode \hat{b} called the RC. This mode is coupled strongly to the system, but weakly to a residual bosonic bath, while conserving the bosonic commutation relations. The new Hamiltonian of the system then becomes

$$\hat{H}_{\text{tot}} = \hat{H} + \lambda \sum_i \hat{S}_i (\hat{b} + \hat{b}^\dagger) + \Omega \hat{b}^\dagger \hat{b} + \hat{H}_{\text{RC-B}} + \hat{H}_{\text{bath}}, \quad (9)$$

where λ is the strength of the coupling between the RC and the system, Ω is the frequency of the RC, $\hat{H}_{\text{RC-B}} = \sum_{k>1} \tilde{g}_k (\hat{b} + \hat{b}^\dagger)(\hat{c}_k + \hat{c}_k^\dagger)$ is the RC-bath coupling Hamiltonian, and \hat{H}_{bath} is the bosonic bath Hamiltonian considered to be identical to the case used in the derivation of Eq. (6), but with one less bosonic mode and with properly transformed coupling coefficients. Thus, the parameters λ and Ω are expressed [85] in terms of the parameters in Eq. (8), $\lambda^2 = \frac{1}{6\pi} \sqrt{\frac{5}{3}} \Gamma \omega_m$ and $\Omega = \sqrt{\frac{5}{3}} \omega_m$, while the spectral function of the residual bath,

$$J'(\omega) = \frac{2\sqrt{5/3} \pi \omega \omega_m^2 n_{\text{BE}}(\omega)}{3\{\pi^2 \omega^2 + 4\omega \text{arctanh}(\omega/\omega_m)[\omega \text{arctanh}(\omega/\omega_m) - 2\omega_m] + 4\omega_m^2\}}, \quad (10)$$

is independent of the original coupling strength Γ . This allows us to derive a QME which has the same form as Eq. (6), but it uses $\hat{H} \mapsto \hat{H} + \lambda \sum_i \hat{S}_i (\hat{b} + \hat{b}^\dagger) + \Omega \hat{b}^\dagger \hat{b}$. Since $\lambda \propto \sqrt{\Gamma}$, the coupling of the system to the RC can be arbitrarily strong without affecting coupling to the residual bath. Despite being time-local, this Lindblad QME including RC captures non-Markovian effects [86]. They, otherwise, require integrodifferential QMEs with a time-retarded kernel [72–74]. In order to reduce the computational complexity for many LSs, an effective Hamiltonian was built by considering [86] only the lowest energy states of the RC; i.e., the matrix representation of \hat{b} is truncated to finite size 15×15 .

Results and discussion. We solve Eq. (6) for Lindbladian dynamics, as well as for non-Markovian dynamics when the RC is included in the Hamiltonian, for FI and AFI chains composed of $N = 4$ sites with periodic boundary conditions hosting spins $S = 1/2$ or $S = 5/2$, as well as $S = 1$ in the Supplemental Material (SM) [87]. The two QMEs are solved using the fourth-order Runge-Kutta method, where $|J| = 1$ sets the unit of energy. For Lindbladian dynamics we use $\Gamma = 0.01|J|$, while for non-Markovian dynamics we use stronger coupling $\Gamma = 0.1|J|$, and the cutoff frequency is chosen as $\omega_m = 3|J|$. Note that choosing a too large ω_m brings the entanglement of LSs to 0 on a very short timescale. The initial condition for the FI is the unentangled pure state $\hat{\rho}(0) = |\Sigma\rangle\langle\Sigma|$, where $|\Sigma\rangle = |\rightarrow\rightarrow\rightarrow\rightarrow\rangle$ with all spins pointing along the x axis. The magnetic field applied for $t \geq 0$, $g\mu_B B_z = 0.8|J|$, is along the z axis. The initial condition for the AFI is the unentangled pure state $\hat{\rho}(0) = |\Omega\rangle\langle\Omega|$, where $|\Omega\rangle = |\sigma_1\sigma_2\sigma_1\sigma_2\rangle$ with $\langle\sigma_{1(2)}|\hat{S}_{1(2)}|\sigma_{1(2)}\rangle$ pointing along $\theta_1 = 1/8$ or $\theta_2 = \pi - 1/8$ and $\phi_{1(2)} = 0$ in spherical coordinates.

In the course of time evolution, $\hat{\rho}(t)$ can become entangled, which is quantified by computing the entanglement negativity [12–16] between the left half (LH) and the right half (RH) of the chain

$$E_N[\hat{\rho}(t)] = \ln \|\hat{\rho}^{\text{TRH}}\|_1 = \ln \sum_n |\lambda_n|, \quad (11)$$

where $\|\hat{A}\|_1 = \text{Tr} \sqrt{\hat{A}^\dagger \hat{A}}$ is the trace norm of the operator \hat{A} , λ_n are the eigenvalues of $\hat{\rho}^{\text{TRH}}$, and the matrix elements of the partial transpose with respect to the RH of the chain are given by $(\hat{\rho}^{\text{TRH}})_{i\alpha;j\beta} = (\hat{\rho})_{j\alpha;i\beta}$. While the standard von Neumann entanglement entropy S_{LH} of half of the chain [7,18] can be nonzero even for the unentangled mixed state in Eq. (2), nonzero E_N necessarily implies entanglement and genuine quantum correlations between the two parts [12–16].

Initially, both the FI and the AFI exhibit dynamical buildup of entanglement signified by $E_N > 0$ in Figs. 1 and 2, respectively. However, Lindbladian dynamics quickly brings $E_N \rightarrow 0$ in the FI hosting $S = 1/2$ [Fig. 1(e)], $S = 1$ (Fig. S1(g) in the SM [87]), and $S = 5/2$ [Fig. 1(g)] spins, as well as in the AFI hosting $S = 5/2$ [Fig. 2(e)] spins. Establishing $E_N \rightarrow 0$ also makes it possible for LLG classical trajectories $\mathbf{S}_i(t)$ to track $\langle\hat{S}_i\rangle(t)$ in Figs. 1, 2, and S1 in the SM [87]. Details of how the LLG equation is solved to obtain $\mathbf{S}_i(t)$, while tuning the Gilbert damping parameter in order to enable comparison of $\mathbf{S}_i(t)$ and $\langle\hat{S}_i\rangle(t)$, are given in the SM [87]. In the AFI case with $S = 1/2$ [Fig. 2(e)] or $S = 1$ (Fig. S1(c) in the SM [87]), entanglement *never* vanishes, $E_N(t) > 0$, even in the long-time limit, thereby maintaining $\langle\hat{S}_i\rangle(t) \neq \mathbf{S}_i(t)$. Thus, we conclude that usage [43,44,46–48,51–58] of the LLG equation in spintronics with AFI layers hosting spins $S = 1/2$

or $S = 1$ cannot be justified microscopically. In the case of non-Markovian dynamics, $E_N(t)$ remains nonzero (Figs. 1, 2, and S1 in the SM [87]) in the FI and the AFI at all times and for $S = 1/2$, $S = 1$, and $S = 5/2$, so that quantum-to-classical transition $\langle \hat{S}_i \rangle(t) \mapsto \mathbf{S}_i(t)$ is never achieved. This then provides an example of how pronounced memory effects can lead to the revival of genuine quantum properties such as quantum coherence, correlations, and entanglement [73].

Finally, we examine the fate of the entangled GS of the AFI upon suddenly coupling it to a bosonic bath and evolving it by the Lindblad equation (6). Let us recall that a common trick employed in TN calculations on spin systems to select the unentangled Néel state as the GS is to introduce an external staggered magnetic field which alternates in sign on atomic length scales [88]. However, its microscopic justification is missing. Attempts to introduce more realistic decoherence mechanisms, such as repeated local measurements [89–91] that would disrupt superposition in the GS and replace the need for the contrived staggered field, are also difficult to justify in the context of spintronic and magnonic devices. A handful of recent studies have examined the time evolution of the entangled GS of AFIs [77,92] upon suddenly coupling their spins to a dissipative environment, but with conflicting conclusions about the fate of entanglement. Since the “checkerboard” pattern of expectation values of $\langle \hat{S}_i \rangle$ in the Néel order is often reported experimentally [41], we induce it as the initial condition at $t = 0$ by using a GS of the slightly modified Heisenberg Hamiltonian

$$\hat{H}_{\text{imp}} = \hat{H}_H - 0.2|J|\hat{S}_1^z, \quad (12)$$

with an additional impurity at site $i = 1$. The impurity breaks the rotational invariance of \hat{H}_H to generate the Néel order,

$\langle \hat{S}_i^z \rangle = -\langle \hat{S}_{i+1}^z \rangle \neq 0$, but not the Néel GS $|\uparrow\downarrow\uparrow\downarrow\rangle$ because the entanglement entropy of the true GS remains nonzero [26] leading to $\langle \hat{S}_i^z \rangle/S < 1$. The Lindbladian time evolution (Fig. 3) maintains the entanglement $E_N(t) > 0$ at low temperature $T_1 = 0.01|J|$ and, therefore, nonclassical dynamics of $\langle \hat{S}_i \rangle(t)$, while at high temperatures $E_N \rightarrow 0$ is reached on short timescales. The overlap $\text{Tr}[\hat{\rho}(t)\hat{P}_{\text{Néel}}]$ with states in the Néel subspace, whose projector is $\hat{P}_{\text{Néel}} = |\uparrow\downarrow\uparrow\downarrow\rangle\langle\uparrow\downarrow\uparrow\downarrow| + |\downarrow\uparrow\downarrow\uparrow\rangle\langle\downarrow\uparrow\downarrow\uparrow|$, never reaches 1 in the low-temperature regime [black curve in Fig. 3(d)]. In the high-temperature limit, the overlap becomes negligible [red curve in Fig. 3(d)] as the system goes [92] into static ferrimagnetic ordering [blue and orange flat lines in Figs. 3(a) and 3(b)].

In conclusion, we solve nearly a century old [59] problem—“unreasonable effectiveness” of the classical LLG equation in describing dynamics of many (for solution of the same problem for a single spin, see Ref. [68]) localized spins within a magnetic material—by showing that it is justified microscopically only if Lindblad open quantum system dynamics is generated by the environment in the case of any ferromagnet, as well as for antiferromagnets with sufficiently large value of their spin $S > 1$. Thus, our findings exclude antiferromagnets with $S = 1/2$ or $S = 1$ spins from the possibility to model them via classical micromagnetics or ASD [69,70]. Our analysis via rigorously constructed Markovian and non-Markovian QMEs for many LSs exhibiting nearly degenerate many-body eigenenergies and interacting with a bosonic bath could also be applied to other related problems, such as the fate of entanglement in quantum spin liquids [93].

Acknowledgments. This research was primarily supported by the U.S. National Science Foundation through the University of Delaware Materials Research Science and Engineering Center, Grant No. DMR-2011824.

-
- [1] N. B. Christensen, H. M. Rønnow, D. F. McMorrow, A. Harrison, T. G. Perring, M. Enderle, R. Coldea, L. P. Regnault, and G. Aeppli, Quantum dynamics and entanglement of spins on a square lattice, *Proc. Natl. Acad. Sci. USA* **104**, 15264 (2007).
 - [2] T. Brydges, A. Elben, P. Jurcevic, B. Vermersch, C. Maier, B. Lanyon, P. Zoller, R. Blatt, and C. Roos, Probing Rényi entanglement entropy via randomized measurements, *Science* **364**, 260 (2019).
 - [3] A. Scheie, P. Laurell, A. M. Samarakoon, B. Lake, S. E. Nagler, G. E. Granroth, S. Okamoto, G. Alvarez, and D. A. Tennant, Witnessing entanglement in quantum magnets using neutron scattering, *Phys. Rev. B* **103**, 224434 (2021).
 - [4] G. Mathew, S. L. L. Silva, A. Jain, A. Mohan, D. T. Adroja, V. G. Sakai, C. V. Tomy, A. Banerjee, R. Goreti, Aswathi V. N., R. Singh, and D. Jaiswal-Nagar, Experimental realization of multipartite entanglement via quantum Fisher information in a uniform antiferromagnetic quantum spin chain, *Phys. Rev. Res.* **2**, 043329 (2020).
 - [5] P. Laurell, A. Scheie, C. J. Mukherjee, M. M. Koza, M. Enderle, Z. Tylczynski, S. Okamoto, R. Coldea, D. A. Tennant, and G. Alvarez, Quantifying and controlling entanglement in the quantum magnet Cs_2CoCl_4 , *Phys. Rev. Lett.* **127**, 037201 (2021).
 - [6] N. Friis, G. Vitagliano, M. Malik, and M. Huber, Entanglement certification from theory to experiment, *Nat. Rev. Phys.* **1**, 72 (2018).
 - [7] G. D. Chiara and A. Sanpera, Genuine quantum correlations in quantum many-body systems: A review of recent progress, *Rep. Prog. Phys.* **81**, 074002 (2018).
 - [8] N. Laflorencie, Quantum entanglement in condensed matter systems, *Phys. Rep.* **646**, 1 (2016).
 - [9] H. F. Song, N. Laflorencie, S. Rachel, and K. Le Hur, Entanglement entropy of the two-dimensional Heisenberg antiferromagnet, *Phys. Rev. B* **83**, 224410 (2011).
 - [10] J. Hales, U. Bajpai, T. Liu, D. R. Baykusheva, M. Li, M. Mitrano, and Y. Wang, Witnessing light-driven entanglement using time-resolved resonant inelastic X-ray scattering, *Nat. Commun.* **14**, 3512 (2023).
 - [11] D. R. Baykusheva, M. H. Kalthoff, D. Hofmann, M. Claassen, D. M. Kennes, M. A. Sentef, and M. Mitrano, Witnessing nonequilibrium entanglement dynamics in a strongly correlated fermionic chain, *Phys. Rev. Lett.* **130**, 106902 (2023).

- [12] A. Peres, Separability criterion for density matrices, *Phys. Rev. Lett.* **77**, 1413 (1996).
- [13] K.-H. Wu, T.-C. Lu, C.-M. Chung, Y.-J. Kao, and T. Grover, Entanglement Renyi negativity across a finite temperature transition: A Monte Carlo study, *Phys. Rev. Lett.* **125**, 140603 (2020).
- [14] A. Elben, R. Kueng, H.-Y. R. Huang, R. van Bijnen, C. Kokail, M. Dalmonte, P. Calabrese, B. Kraus, J. Preskill, P. Zoller, and B. Vermersch, Mixed-state entanglement from local randomized measurements, *Phys. Rev. Lett.* **125**, 200501 (2020).
- [15] S. Sang, Y. Li, T. Zhou, X. Chen, T. H. Hsieh, and M. P. A. Fisher, Entanglement negativity at measurement-induced criticality, *PRX Quantum* **2**, 030313 (2021).
- [16] L. Aolita, F. de Melo, and L. Davidovich, Open-system dynamics of entanglement: A key issues review, *Rep. Prog. Phys.* **78**, 042001 (2015).
- [17] M. C. Bañuls, Tensor network algorithms: A route map, *Annu. Rev. Condens. Matter Phys.* **14**, 173 (2023).
- [18] J. H. Bardarson, F. Pollmann, and J. E. Moore, Unbounded growth of entanglement in models of many-body localization, *Phys. Rev. Lett.* **109**, 017202 (2012).
- [19] R. Trivedi and J. I. Cirac, Transitions in computational complexity of continuous-time local open quantum dynamics, *Phys. Rev. Lett.* **129**, 260405 (2022).
- [20] A. Lerose, M. Sonner, and D. A. Abanin, Overcoming the entanglement barrier in quantum many-body dynamics via space-time duality, *Phys. Rev. B* **107**, L060305 (2023).
- [21] S. Sahling, G. Remenyi, C. Paulsen, P. Monceau, V. Saligrama, C. Marin, A. Revcolevschi, L. P. Regnault, S. Raymond, and J. E. Lorenzo, Experimental realization of long-distance entanglement between spins in antiferromagnetic quantum spin chains, *Nat. Phys.* **11**, 255 (2015).
- [22] F. H. L. Essler, H. Frahm, F. Göhmann, A. Klümper, and V. E. Korepin, *The One-Dimensional Hubbard Model* (Cambridge University, Cambridge, England, 2005).
- [23] A. Singh and Z. Tešanović, Quantum spin fluctuations in an itinerant antiferromagnet, *Phys. Rev. B* **41**, 11457 (1990).
- [24] R. Wieser, Description of a dissipative quantum spin dynamics with a Landau-Lifshitz/Gilbert like damping and complete derivation of the classical Landau-Lifshitz equation, *Eur. Phys. J. B* **88**, 77 (2015).
- [25] P. Mondal, A. Suresh, and B. K. Nikolić, When can localized spins interacting with conduction electrons in ferro- or antiferromagnets be described classically via the Landau-Lifshitz equation: Transition from quantum many-body entangled to quantum-classical nonequilibrium states, *Phys. Rev. B* **104**, 214401 (2021).
- [26] M. D. Petrović, P. Mondal, A. E. Feiguin, and B. K. Nikolić, Quantum spin torque driven transmutation of an antiferromagnetic Mott insulator, *Phys. Rev. Lett.* **126**, 197202 (2021).
- [27] J. S. Pratt, Universality in the entanglement structure of ferromagnets, *Phys. Rev. Lett.* **93**, 237205 (2004).
- [28] U. Bajpai, A. Suresh, and B. K. Nikolić, Quantum many-body states and Green's functions of nonequilibrium electron-magnon systems: Localized spin operators versus their mapping to Holstein-Primakoff bosons, *Phys. Rev. B* **104**, 184425 (2021).
- [29] H. Yuan, Y. Cao, A. Kamra, R. A. Duine, and P. Yan, Quantum magnonics: When magnon spintronics meets quantum information science, *Phys. Rep.* **965**, 1 (2022).
- [30] T. Morimae, A. Sugita, and A. Shimizu, Macroscopic entanglement of many-magnon states, *Phys. Rev. A* **71**, 032317 (2005).
- [31] D. Lachance-Quirion, S. P. Wolski, Y. Tabuchi, S. Kono, K. Usami, and Y. Nakamura, Entanglement-based single-shot detection of a single magnon with a superconducting qubit, *Science* **367**, 425 (2020).
- [32] J. S. Pratt, Qubit entanglement in multimagnon states, *Phys. Rev. B* **73**, 184413 (2006).
- [33] A. R. R. Carvalho, F. Mintert, and A. Buchleitner, Decoherence and multipartite entanglement, *Phys. Rev. Lett.* **93**, 230501 (2004).
- [34] H. Y. Yuan, W. P. Sterk, A. Kamra, and R. A. Duine, Master equation approach to magnon relaxation and dephasing, *Phys. Rev. B* **106**, 224422 (2022).
- [35] H. Y. Yuan, W. P. Sterk, A. Kamra, and R. A. Duine, Pure dephasing of magnonic quantum states, *Phys. Rev. B* **106**, L100403 (2022).
- [36] V. Azimi Mousolou, A. Bagrov, A. Bergman, A. Delin, O. Eriksson, Y. Liu, M. Pereiro, D. Thonig, and E. Sjöqvist, Hierarchy of magnon mode entanglement in antiferromagnets, *Phys. Rev. B* **102**, 224418 (2020).
- [37] V. Baltz, A. Manchon, M. Tsoi, T. Moriyama, T. Ono, and Y. Tserkovnyak, Antiferromagnetic spintronics, *Rev. Mod. Phys.* **90**, 015005 (2018).
- [38] T. Jungwirth, X. Marti, P. Wadley, and J. Wunderlich, Antiferromagnetic spintronics, *Nat. Nanotechnol.* **11**, 231 (2016).
- [39] J. Železný, P. Wadley, K. Olejník, A. Hoffmann, and H. Ohno, Spin transport and spin torque in antiferromagnetic devices, *Nat. Phys.* **14**, 220 (2018).
- [40] M. B. Jungfleisch, W. Zhang, and A. Hoffmann, Perspectives of antiferromagnetic spintronics, *Phys. Lett. A* **382**, 865 (2018).
- [41] I. Gray, T. Moriyama, N. Sivadas, G. M. Stiehl, J. T. Heron, R. Need, B. J. Kirby, D. H. Low, K. C. Nowack, D. G. Schlom, D. C. Ralph, T. Ono, and G. D. Fuchs, Spin Seebeck imaging of spin-torque switching in antiferromagnetic Pt/NiO heterostructures, *Phys. Rev. X* **9**, 041016 (2019).
- [42] U. Ritzmann, P. Baláž, P. Maldonado, K. Carva, and P. M. Oppeneer, High-frequency magnon excitation due to femtosecond spin-transfer torques, *Phys. Rev. B* **101**, 174427 (2020).
- [43] A. Suresh, M. D. Petrović, U. Bajpai, H. Yang, and B. K. Nikolić, Magnon- versus electron-mediated spin-transfer torque exerted by spin current across an antiferromagnetic insulator to switch the magnetization of an adjacent ferromagnetic metal, *Phys. Rev. Appl.* **15**, 034089 (2021).
- [44] R. Cheng, J. Xiao, Q. Niu, and A. Brataas, Spin pumping and spin-transfer torques in antiferromagnets, *Phys. Rev. Lett.* **113**, 057601 (2014).
- [45] Y. Wang, D. Zhu, Y. Yang, K. Lee, R. Mishra, G. Go, S.-H. Oh, D.-H. Kim, K. Cai, E. Liu, S. D. Pollard, S. Shi, J. Lee, K. L. Teo, Y. Wu, K.-J. Lee, and H. Yang, Magnetization switching by magnon-mediated spin torque through an antiferromagnetic insulator, *Science* **366**, 1125 (2019).
- [46] A. V. Kimel, B. A. Ivanov, R. V. Pisarev, P. A. Usachev, A. Kirilyuk, and T. Rasing, Inertia-driven spin switching in antiferromagnets, *Nat. Phys.* **5**, 727 (2009).
- [47] T. Kampfrath, A. Sell, G. Klatt, A. Pashkin, S. Mährlein, T. Dekorsy, M. Wolf, M. Fiebig, A. Leitenstorfer, and R. Huber,

- Coherent terahertz control of antiferromagnetic spin waves, *Nat. Photon.* **5**, 31 (2011).
- [48] P. Vaidya, S. A. Morley, J. van Tol, Y. Liu, R. Cheng, A. Brataas, D. Lederman, and E. del Barco, Subterahertz spin pumping from an insulating antiferromagnet, *Science* **368**, 160 (2020).
- [49] J. Li, C. B. Wilson, R. Cheng, M. Lohmann, M. Kavand, W. Yuan, M. Aldosary, N. Agladze, P. Wei, M. S. Sherwin, and J. Shi, Spin current from sub-terahertz-generated antiferromagnetic magnons, *Nature (London)* **578**, 70 (2020).
- [50] H. Qiu, L. Zhou, C. Zhang, J. Wu, Y. Tian, S. Cheng, S. Mi, H. Zhao, Q. Zhang, D. Wu, B. Jin, J. Chen, and P. Wu, Ultrafast spin current generated from an antiferromagnet, *Nat. Phys.* **17**, 388 (2021).
- [51] G. M. Diederich, J. Cenker, Y. Ren, J. Fonseca, D. G. Chica, Y. J. Bae, X. Zhu, X. Roy, T. Cao, D. Xiao, and X. Xu, Tunable interaction between excitons and hybridized magnons in a layered semiconductor, *Nat. Nanotech.* **18**, 23 (2022).
- [52] Y. Sun, F. Meng, C. Lee, A. Soll, H. Zhang, R. Ramesh, J. Yao, Z. Sofer, and J. Orenstein, Dipolar spin wave packet transport in a van der Waals antiferromagnet, *Nat. Phys.* (2024), doi:10.1038/s41567-024-02387-2.
- [53] H. Y. Yuan, Q. Liu, K. Xia, Z. Yuan, and X. R. Wang, Proper dissipative torques in antiferromagnetic dynamics, *Europhys. Lett.* **126**, 67006 (2019).
- [54] F. L. A. Machado, P. R. T. Ribeiro, J. Holanda, R. L. Rodríguez-Suárez, A. Azevedo, and S. M. Rezende, Spin-flop transition in the easy-plane antiferromagnet nickel oxide, *Phys. Rev. B* **95**, 104418 (2017).
- [55] P. Li, J. Chen, R. Du, and X.-P. Wang, Numerical methods for antiferromagnets, *IEEE Trans. Magn.* **56**, 1 (2020).
- [56] R. Mondal, S. Großenbach, L. Rózsa, and U. Nowak, Nutation in antiferromagnetic resonance, *Phys. Rev. B* **103**, 104404 (2021).
- [57] R. Mondal and L. Rózsa, Inertial spin waves in ferromagnets and antiferromagnets, *Phys. Rev. B* **106**, 134422 (2022).
- [58] P. Dhali and R. Mondal, Theory of tensorial Gilbert damping in antiferromagnets, *J. Phys. Condens. Matter* **36**, 255804 (2024).
- [59] L. D. Landau and E. M. Lifshitz, On the theory of the dispersion of magnetic permeability in ferromagnetic bodies, *Phys. Z. Sowjetunion* **8**, 153 (1935).
- [60] T. Gilbert, A phenomenological theory of damping in ferromagnetic materials, *IEEE Trans. Magn.* **40**, 3443 (2004).
- [61] W. M. Saslow, Landau–Lifshitz or Gilbert damping? That is the question, *J. Appl. Phys.* **105**, 07D315 (2009).
- [62] J. Gauryacq and N. Lorente, Classical limit of a quantal nanomagnet in an anisotropic environment, *Surf. Sci.* **630**, 325 (2014).
- [63] J. L. García-Palacios and D. Zueco, Solving spin quantum master equations with matrix continued-fraction methods: Application to superparamagnets, *J. Phys. A: Math. Theor.* **39**, 13243 (2006).
- [64] R. Wieser, Comparison of quantum and classical relaxation in spin dynamics, *Phys. Rev. Lett.* **110**, 147201 (2013).
- [65] J. B. Parkinson, J. C. Bonner, G. Müller, M. P. Nightingale, and H. W. J. Blöte, Heisenberg spin chains: Quantum-classical crossover and the Haldane conjecture, *J. Appl. Phys.* **57**, 3319 (1985).
- [66] E. Kaxiras and J. D. Joannopoulos, *Quantum Theory of Materials* (Cambridge University, Cambridge, England, 2019).
- [67] A. J. Leggett, S. Chakravarty, A. T. Dorsey, M. P. A. Fisher, A. Garg, and W. Zwerger, Dynamics of the dissipative two-state system, *Rev. Mod. Phys.* **59**, 1 (1987).
- [68] J. Anders, C. Sait, and S. Horsley, Quantum Brownian motion for magnets, *New J. Phys.* **24**, 033020 (2022).
- [69] R. F. L. Evans, W. J. Fan, P. Chureemart, T. A. Ostler, M. O. A. Ellis, and R. W. Chantrell, Atomistic spin model simulations of magnetic nanomaterials, *J. Phys.: Condens. Matter* **26**, 103202 (2014).
- [70] S.-K. Kim, Micromagnetic computer simulations of spin waves in nanometre-scale patterned magnetic elements, *J. Phys. D: Appl. Phys.* **43**, 264004 (2010).
- [71] M. D. Petrović, P. Mondal, A. E. Feiguin, P. Plecháč, and B. K. Nikolić, Spintronics meets density matrix renormalization group: Quantum spin-torque-driven nonclassical magnetization reversal and dynamical buildup of long-range entanglement, *Phys. Rev. X* **11**, 021062 (2021).
- [72] H.-P. Breuer and F. Petruccione, *The Theory of Open Quantum Systems* (Oxford University, Oxford, 2007).
- [73] H.-P. Breuer, E.-M. Laine, J. Piilo, and B. Vacchini, Colloquium: Non-Markovian dynamics in open quantum systems, *Rev. Mod. Phys.* **88**, 021002 (2016).
- [74] I. de Vega and D. Alonso, Dynamics of non-Markovian open quantum systems, *Rev. Mod. Phys.* **89**, 015001 (2017).
- [75] F. Nathan and M. S. Rudner, Universal Lindblad equation for open quantum systems, *Phys. Rev. B* **102**, 115109 (2020).
- [76] G. Schaller, *Open Quantum Systems Far from Equilibrium* (Springer, Cham, 2014).
- [77] M. Weber, D. J. Luitz, and F. F. Assaad, Dissipation-induced order: The $S = 1/2$ quantum spin chain coupled to an Ohmic bath, *Phys. Rev. Lett.* **129**, 056402 (2022).
- [78] D. Manzano, A short introduction to the Lindblad master equation, *AIP Adv.* **10**, 025106 (2020).
- [79] G. Lindblad, On the generators of quantum dynamical semigroups, *Commun. Math. Phys.* **48**, 119 (1976).
- [80] A. Norambuena, A. Franco, and R. Coto, From the open generalized Heisenberg model to the Landau–Lifshitz equation, *New J. Phys.* **22**, 103029 (2020).
- [81] G. B. Cuetara, M. Esposito, and G. Schaller, Quantum thermodynamics with degenerate eigenstate coherences, *Entropy* **18**, 447 (2016).
- [82] E. Mozgunov and D. Lidar, Completely positive master equation for arbitrary driving and small level spacing, *Quantum* **4**, 227 (2020).
- [83] G. McCauley, B. Cruikshank, D. I. Bondar, and K. Jacobs, Accurate Lindblad-form master equation for weakly damped quantum systems across all regimes, *npj Quantum Inf.* **6**, 74 (2020).
- [84] G. T. Landi, D. Poletti, and G. Schaller, Nonequilibrium boundary-driven quantum systems: Models, methods, and properties, *Rev. Mod. Phys.* **94**, 045006 (2022).
- [85] A. Nazir and G. Schaller, The reaction coordinate mapping in quantum thermodynamics, in *Thermodynamics in the Quantum Regime: Fundamental Aspects and New Directions*, edited by F. Binder, L. A. Correa, C. Gogolin, J. Anders, and G. Adesso (Springer, Cham, 2018), pp. 551–577.

- [86] N. Anto-Sztrikacs and D. Segal, Strong coupling effects in quantum thermal transport with the reaction coordinate method, *New J. Phys.* **23**, 063036 (2021).
- [87] See Supplemental Material at <http://link.aps.org/supplemental/10.1103/PhysRevB.109.L180408> for additional Fig. S1 as the counterpart of Figs. 1 and 2, but considering $S = 1$ LS within either FI or AFI chains; numerical procedures for solving the LLG equation for $\mathbf{S}_i(t)$, as well as for comparing $\mathbf{S}_i(t)$ with $\langle \hat{\mathbf{S}}_i \rangle(t)$, which also allows one to extract *microscopically* the Gilbert damping in the LLG equation; the effect of additional interactions acting on LS, such as easy-axis anisotropy, dipole-dipole interaction, and Dzyaloshinskii-Moriya interaction; usage of a single vs many independent bosonic baths; exploration of wide range of temperatures of bosonic baths; proximity of steady-state solution of the Lindblad QME to Gibbs density matrix describing thermal equilibrium; and scaling of entanglement with increasing number of spins, and which includes Refs. [94–110].
- [88] E. Stoudenmire and S. R. White, Studying two-dimensional systems with the density matrix renormalization group, *Annu. Rev. Condens. Matter Phys.* **3**, 111 (2012).
- [89] M. I. Katsnelson, V. V. Dobrovitski, and B. N. Harmon, Néel state of an antiferromagnet as a result of a local measurement in the distributed quantum system, *Phys. Rev. B* **63**, 212404 (2001).
- [90] H. C. Donker, H. De Raedt, and M. I. Katsnelson, Decoherence wave in magnetic systems and creation of Néel antiferromagnetic state by measurement, *Phys. Rev. B* **93**, 184426 (2016).
- [91] H. C. Donker, H. De Raedt, and M. I. Katsnelson, Antiferromagnetic order without recourse to staggered fields, *Phys. Rev. B* **98**, 014416 (2018).
- [92] G. Schaller, F. Queisser, N. Szpak, J. König, and R. Schützhold, Environment-induced decay dynamics of antiferromagnetic order in Mott-Hubbard systems, *Phys. Rev. B* **105**, 115139 (2022).
- [93] K. Yang, S. C. Morampudi, and E. J. Bergholtz, Exceptional spin liquids from couplings to the environment, *Phys. Rev. Lett.* **126**, 077201 (2021).
- [94] A. Szilva, Y. Kvashnin, E. A. Stepanov, L. Nordström, O. Eriksson, A. I. Lichtenstein, and M. I. Katsnelson, Quantitative theory of magnetic interactions in solids, *Rev. Mod. Phys.* **95**, 035004 (2023).
- [95] R. P. Erickson, Long-range dipole-dipole interactions in a two-dimensional Heisenberg ferromagnet, *Phys. Rev. B* **46**, 14194 (1992).
- [96] M. Sharma, Govind, A. Pratap, Ajay, and R. Tripathi, Role of dipole-dipole interaction on the magnetic dynamics of anisotropic layered cuprate antiferromagnets, *Phys. Status Solidi B* **226**, 193 (2001).
- [97] E. Davis, B. Ye, F. Machado, S. Meynell, W. Wu, T. Mittiga, W. Schenken, M. Joos, B. Kobrin, Y. Lyu, Z. Wang, D. Bluvstein, S. Choi, C. Zu, A. Jayich, and N. Yao, Probing many-body dynamics in a two-dimensional dipolar spin ensemble, *Nat. Phys.* **19**, 836 (2023).
- [98] B. Sbierski, M. Bintz, S. Chatterjee, M. Schuler, N. Y. Yao, and L. Pollet, Magnetism in the two-dimensional dipolar XY model, *Phys. Rev. B* **109**, 144411 (2024).
- [99] R. E. Camley and K. L. Livesey, Consequences of the Dzyaloshinskii-Moriya interaction, *Surf. Sci. Rep.* **78**, 100605 (2023).
- [100] T. Prosen, Exact nonequilibrium steady state of an open Hubbard chain, *Phys. Rev. Lett.* **112**, 030603 (2014).
- [101] F. Queisser and R. Schützhold, Environment-induced pre-relaxation in the Mott-Hubbard model, *Phys. Rev. B* **99**, 155110 (2019).
- [102] J. S. Lee and J. Yeo, Comment on “Universal Lindblad equation for open quantum systems,” *arXiv:2011.00735*.
- [103] F. Nathan and M. S. Rudner, High accuracy steady states obtained from the universal Lindblad equation, *arXiv:2206.02917*.
- [104] J. L. García-Palacios and F. J. Lázaro, Langevin-dynamics study of the dynamical properties of small magnetic particles, *Phys. Rev. B* **58**, 14937 (1998).
- [105] J. Zou, S. K. Kim, and Y. Tserkovnyak, Tuning entanglement by squeezing magnons in anisotropic magnets, *Phys. Rev. B* **101**, 014416 (2020).
- [106] F. Iemini, D. Chang, and J. Marino, Dynamics of inhomogeneous spin ensembles with all-to-all interactions: Breaking permutational invariance, *Phys. Rev. A* **109**, 032204 (2024).
- [107] A. Seif, Y.-X. Wang, and A. A. Clerk, Distinguishing between quantum and classical Markovian dephasing dissipation, *Phys. Rev. Lett.* **128**, 070402 (2022).
- [108] M. A. Nielsen and I. L. Chuang, *Quantum Computation and Quantum Information: 10th Anniversary Edition* (Cambridge University, Cambridge, England, 2010).
- [109] J. D. Cresser and J. Anders, Weak and ultrastrong coupling limits of the quantum mean force Gibbs state, *Phys. Rev. Lett.* **127**, 250601 (2021).
- [110] A. Schuckert, A. Pineiro Orioli, and J. Berges, Nonequilibrium quantum spin dynamics from two-particle irreducible functional integral techniques in the Schwinger boson representation, *Phys. Rev. B* **98**, 224304 (2018).